Avalanche photo-detection for high data rate applications

H B Coldenstrodt-Ronge[1,2] and C Silberhorn[1]

[1] Max-Planck Research Group, Günther-Scharowskystrasse 1/Bau 24, 91058 Erlangen, Germany
[2] Clarendon Laboratory, University of Oxford, Parks Road, Oxford, OX1 3PU, UK

E-mail: csilberhorn@optik.uni-erlangen.de

Abstract
Avalanche photo-detection is commonly used in applications which require single-photon sensitivity. We examine the limits of using avalanche photo-diodes (APD) for characterizing photon statistics at high data rates. To identify the regime of linear APD operation, we employ a ps-pulsed diode laser with variable repetition rates between 0.5 MHz and 80 MHz. We modify the mean optical power of the coherent pulses by applying different levels of well-calibrated attenuation. The linearity at high repetition rates is limited by the APD dead time and a nonlinear response arises at higher photon-numbers due to multiphoton events. Assuming Poissonian input-light statistics we ascertain the effective mean photon-number of the incident light with high accuracy. Time multiplexed detectors (TMD) allow us to accomplish photon-number resolution by 'photon chopping'. This detection setup extends the linear response function to higher photon-numbers and statistical methods may be used to compensate for nonlinearity. We investigate this effect, compare it to the single APD case and show the validity of the convolution treatment in the TMD data analysis.

1. Introduction

Studying distinct quantum properties of light has initiated a multitude of new developments in quantum optics and fundamental physics. In recent decades it has actually triggered the evolution of quantum technologies and quantum communication, which are based on genuine quantum effects that have no classical counterpart. For such applications the interest in the performance of detectors has shifted: while for fundamental research the quantum efficiency essentially defines solely the quality of a measurement setup, the benchmark for detectors in quantum communication systems also comprises the experimental complexity, detector noise and the maximum speed of possible data rates in single-shot operation (Bienfang *et al* 2004, Gordon *et al* 2005, Thew *et al* 2006, Takesue *et al* 2006).

Two general approaches are currently in use to characterize quantum states in communication systems: single-photon schemes rely on avalanche photo-diodes, while continuous variable (CV) systems employ homodyne detection. Time-resolved homodyne detection setups utilize conventional photo-diodes to realize single-shot measurements of quadrature uncertainties (Smithey *et al* 1993, Raymer *et al* 1995, Hansen *et al* 2001, Zavatta *et al* 2002, Wenger *et al* 2004). Thus, CV communication promises quantum key exchange at high repetition rates (Grosshans *et al* 2002, Hirano *et al* 2003, Lance *et al* 2005, Lorenz *et al* 2006); though it requires a more intricate data post-processing with reduced sifted secure bit rates. In contrast, various techniques have been realized up-to-date to observe single photons: photomultiplier tubes, avalanche photo-diodes (APDs), visible light photon counters (VLPCs) and superconducting sensors, like the superconducting edge sensor or superconducting bolometers (Cabrera *et al* 1998, Fujiwara and Sasaki 2006, Hadfield *et al* 2005, Kim *et al* 1999, Rosenberg *et al* 2005, Somani *et al* 2001). In the visible regime avalanche photo-diodes however combine reasonable quantum efficiencies of about 60% and comparatively low dark-count noise with an operation at room temperature and commercial availability. Neglecting the difference in quantum efficiency, the APDs seem to gather many advantages, but unfortunately they are binary detectors. Thus they are not capable to distinguish directly between different photon-numbers. In order to achieve photon-number resolution with APDs, schemes as 'photon chopping', e.g., by beam splitters (Paul *et al* 1996, Kok and Braunstein 2001), or time-multiplexing have been proposed and implemented (Banaszek and Walmsley 2003, Fitch *et al* 2003, Achilles *et al* 2004). The basic idea is to split the pulse under investigation into several pulses and to measure them subsequently with APDs. The influence of losses and their treatment in the data analysis have been theoretically and experimentally investigated in previous work (Achilles *et al* 2004, 2006). Further distortion of measurement results arises from photons, which are not separated into different bins and thus get still masked by the non-photon resolving nature of the APD. For the characterization of photonic states with one single APD multi-photon contributions have been assessed by attenuation measurements with variable quantum efficiencies. In principle, this method allows the complete reconstruction of the photon-number statistics (Wenger *et al* 2004, Zambra *et al* 2005).

In this paper, we investigate the limits of characterizing photon statistics with commercial APDs at 800 nm for moderate to high bit rate applications. In this context, a specific parameter of the APDs is their dead time, which ultimately restricts the speed quantum systems can be driven at. Other schemes have suggested to use active, high-speed switches in combination with an APD array to overcome correction which arises from detector dead time (Castelletto *et al* 2006). Our attempt is to keep the complexity of the detection to a minimum by utilizing pico-second pulsed light at appropriate repetition rates to lessen dead-time limitations. Furthermore, for pulsed systems dark-count contributions can be largely suppressed by applying a narrow time gating. This is only limited by the jitter of the APDs and the duration of the light pulses. The full characterization of APDs involves their count-rate response, dark counts, dead times after a detection event and the detection efficiency. Methods of measuring the quantum efficiency of APDs have been proposed and are well established (Klyshko 1977a, 1977b, Rarity *et al* 1987, Penin and Sergienko 1991, Ware and Migdall 2004). However, they do not consider effects arising from the dead times for higher count rates.

We use only passive optical elements and restrict the number of APDs to two. In all experimental configurations we employed coherent light with different intensities, repetition rates and pulse power. While for cw-light the monitored count rates can only be modified by changing the intensity, pulsed light also allows us to control the time slots of possible detection events. For comparison, we start our analysis by recording the APD response in

dependency on well-calibrated intensities of cw-light. We then perform different measurement sets in the pulsed regime with variable repetition rates to separate dead-time effects from the influence of multi-photon contributions of the incident light. For photon-number resolved measurements with time-multiplexed detection (TMD) the theoretical treatment of higher number contributions is given in Achilles *et al* (2004). We show experimentally that for higher power levels the inclusion of the described convolution effect is essential for the apt interpretation of measured data. Though appropriate theoretical modelling enables a reliable reconstruction of impinging photon statistics. This complements the experimental TMD detector characterization and shows in combination with the loss inversion (Achilles *et al* 2006), the capability of TMDs for quantum communication systems.

2. Theory of APD photo-detection

Due to the charge carrier avalanche in the detection process, APDs can resolve individual photons, but as a drawback they saturate already at the single-photon level. This binary response reads: either no detection event (NO CLICK) or at least one photon is detected (CLICK). The corresponding POVM elements are given by $\mathbb{1} - |0\rangle\langle 0|$ and $|0\rangle\langle 0|$, respectively. As long as the photons arrive at the detector individually and well separated in time, the detected counts scale linearly with the number of incident photons as intuitively expected. Timing control can be ensured in the pulsed regime. The response of a binary detector then depends only on the probability that at least one photon is present in an incident pulse. This probability is given by $P_1 = 1 - P_0$, where P_0 denotes the probability that the input light contains no photon. For a detector with quantum efficiency η_{APD} and a dark-count rate R_{dark} we can calculate an expected count rate of

$$R_{\mathrm{cnt}} = f_{\mathrm{rep}}\eta_{\mathrm{APD}}\left(1 - P_0\right) + R_{\mathrm{dark}}, \tag{1}$$

if a pulse repetition frequency f_{rep} is assumed for the input signal states.

In order to characterize the responding behaviour of the APDs, we have to ensure that we control precisely the influence of the photon statistics of the input light. We used coherent light which is represented in the photon-number basis as

$$|\alpha\rangle = \sum_n \exp\left(-\frac{|\alpha|^2}{2}\right)\frac{\alpha^n}{\sqrt{n!}}|n\rangle, \tag{2}$$

i.e. it obeys a Poissonian photon-number distribution. As usual we model the attenuation $1 - \eta^2$ as a beam splitter such that the coherent state transforms like

$$\hat{U}_\eta|\alpha\rangle = |\eta\alpha\rangle = \sum_n \exp\left(-\frac{|\eta\alpha|^2}{2}\right)\frac{(\eta\alpha)^n}{\sqrt{n!}}|n\rangle. \tag{3}$$

The probability for no photons present in a pulse is then given by

$$P_0 = \exp(-|\eta|^2|\alpha|^2). \tag{4}$$

Assuming a constant quantum efficiency of the APDs, (1) rewrites to

$$\tilde{R}_{\mathrm{cnt}} = f_{\mathrm{rep}}(1 - \exp(-|\eta|^2|\alpha|^2)) + \tilde{R}_{\mathrm{dark}}, \tag{5}$$

with effective values $\tilde{R}_{\mathrm{cnt}}$ and $\tilde{R}_{\mathrm{dark}}$.

If the influences on the count rates are known, a count-rate-dependent correction factor $C(R_{\mathrm{measured}})$ can be introduced. With knowledge of the correction factor the real count rates R_{real} can be determined from the measured count rates R_{measured}:

$$C(R_{\mathrm{measured}}) = \frac{R_{\mathrm{real}}}{R_{\mathrm{measured}}}. \tag{6}$$
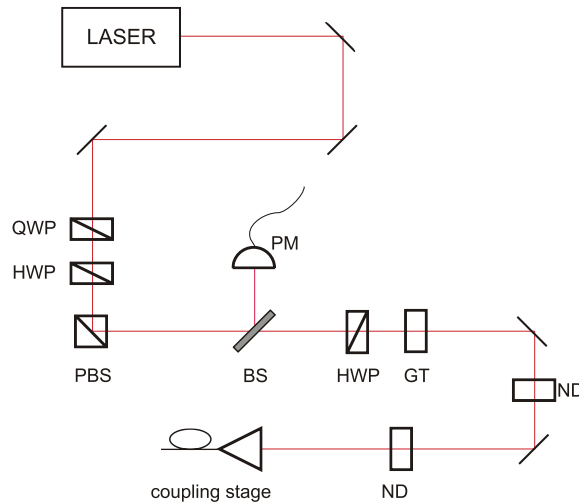
Figure 1. Scheme of the optical setup we used for characterizing the APDs in cw and pulsed operation: QWP, quarter-wave plate; HWP, half-wave plate; PBS, polarizing beam splitter; BS, beam sampler; PM, power meter; GT, Glan–Thompson polarizer; ND, neutral density filter.

The designation of this factor depends on the calibration of the real photon-number. We explored different possibilities to retrieve the real input photon-numbers for high count rates including the data sheets provided by the manufacturer for the specific APD modules.

3. Optical setup

The general experimental setup is illustrated in figure 1. We employed a PicoQuant diode laser system (PDL-800B) for the generation of pulsed coherent states. Our system permitted adjustable repetition rates between 1 and 80 MHz and delivered ps-pulses with a centre frequency at $\bar{\lambda}_{centre} \approx 805.3$ nm. The maximum mean power reached up to 1 mW. To realize the cw-case we used a diode laser with an optical output power of $P_{cw} \approx 8$ mW at the centre frequency $\lambda = 800$ nm. For most measurements we utilized a half-wave plate in combination with a polarizing beam splitter to implement a variable attenuation with a dynamical extinction ratio of around 1:35. For the measurements with the cw-laser we used an additional Glan–Thompson polarizer, which allowed to access an extinction ratio of more than 1:300. To ascertain the attenuation factor, part of the light was reflected out by a beam sampler with constant splitting ratio and monitored by a power meter. In the signal arm, a fixed attenuation of several orders of magnitude was necessary to reduce the laser power down to the low photon-number regime. Hereby, special care had to be taken to suppress reflection and interferences between the neutral density filters. These could otherwise falsify the calibration for different filter sets needed to change the mean optical powers. Furthermore, the power meter used to measure the attenuation showed offsets between its different linearity regimes. Hence, all measurements had to be taken with one fixed filter setting and a sufficiently high range of variable attenuation. Finally, the signal light was coupled into a multimode patchcord fibre cable, connected to the APD modules (Perkin&Elmer SPCM-AQR-13-FC) and a computer-based counter card was used to monitor the resulting count rates.
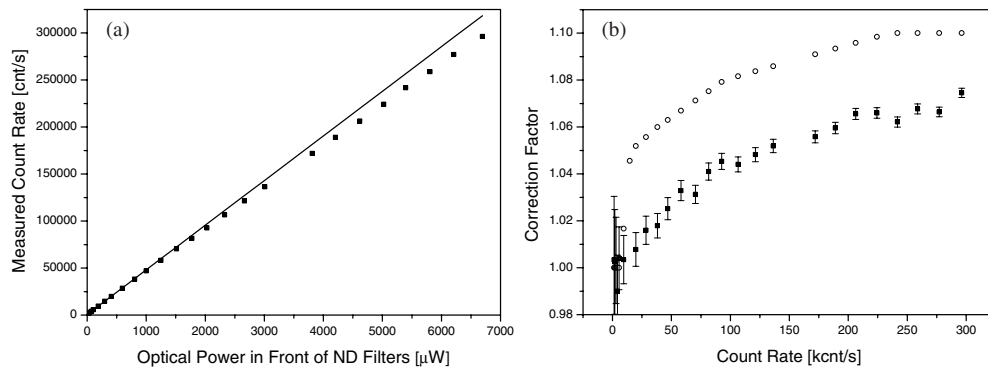
Figure 2. (a) Measured count rate for cw-light against optical power, i.e. transmission of the variable attenuation. The linear fit is included and for higher count rates a significant deviation of the measured data from a linear dependency is visible. The errors in the measured count rates are too small to be visible in the graph. (b) The correction factor calculated according to (6) against the measured count rate (■) in comparison to interpolated values from the data sheet (○).

4. Experimental results

Before recording the data sets for the count rates of various experimental configurations we determined the APD dead times by taking a histogram of the time difference between two consecutive electronic signals produced by the APDs. We found a measured APD dead time of ≈ 53 ns, which was independent of the count rates. With the APDs in a shielding box, we measured the count rates without any incident light. This absolute dark-count level was well below the specified limit of 250 cnt s^{-1}.

4.1. CW-light

According to their data sheet (SPCM-AQR 2005), APDs show the first signs of a nonlinear response at count rates as low as 15.5 kcnt s^{-1}. Hereby, the manufacturer implicitly assumes cw input light. We recorded APD count rates for cw-light at different levels of calibrated attenuation and observed increasing count rates up to 296 kcnt s^{-1}. In this regime a noticeable correction is already expected. In figure 2, we plot the measured count rates against the optical power, i.e. the transmission of the variable attenuation. At low power levels a linear dependency is confirmed such that we can specify a linearity regime for count rates up to 6.5 kcnt s^{-1}. The corresponding linear fit is included in the graph. At higher optical power, the measured count rates are significantly lower than predicted by the fit. The estimated mean photon-number—estimated by the observed optical powers at the monitoring power meter—is still very low, such that the probability of multi-photon events is negligible at these low count rates.

The discrepancy of these observed count rates from the linear behaviour can thus not be explained by multi-photon contributions. If we assume that only the zero-photon and single-photon components are significant, we can use the linear fit to evaluate the real count rate R_{real}. According to (6), we can now estimate the correction factor C for our experimental data and compare it with the values given in the data sheet of the manufacturer. Figure 2 depicts the corresponding correction factors in dependence of the detected count rates. Our experimental measurement results show the same general features as the APD data sheet, but they appear to be lower than the specified correction factors of the manufacturer. The instability of the
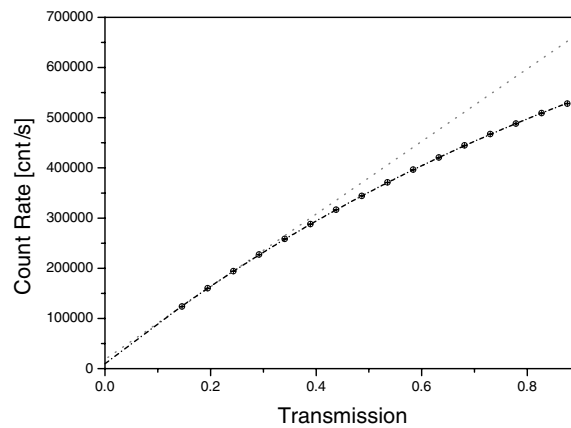
Figure 3. Measured count rates for pulsed light at constant repetition frequency against transmission of the variable attenuator (○). For low transmission a linear fit (grey, dotted) is still a valid approximation, while for higher transmission the photon-number distribution and binary nature of the detector must be taken into account. A fit following (5) is included (black, dot-line) and shows good agreement with the measured data. The errors in the measured count rates are too small to be visible in the graph.

measured values and the global offset are likely to be due to difficulties in the calibration of the *absolute* power level for the extremely low light levels we operated at. Note by comparing the equations (2) and (3) that the attenuation of a coherent state yields another coherent state with reduced field amplitude. If the APD detection efficiency is not exactly known, it is only possible to determine the absolute value of field amplitude α of the coherent input state up to the factor η_{det}. Since the manufacturers only specify a minimum $\eta_{APD}^{\min}$ and moreover a precise assessment of the coupling losses is also extremely difficult in this power regime, we have to introduce an effective detection loss parameter η_{det} to include unspecified coupling and APD efficiencies.

The early nonlinearity for the estimated low power level evinces that other effects than the high photon-number contributions cause the nonlinear behaviour. For cw-light the arrival times of the photons are not restricted to specific time slots. After each detection event the APDs are blocked for the duration of their dead time and pulses arriving in this period are not counted. This can happen at any count rate, independently of the higher order photon-numbers and gives rise to the early nonlinearity.

4.2. Pulsed light at constant repetition frequency

In order to distinguish the impact of the APD dead times on the count rates from the nonlinear response caused by the photon-number statistics of the input light, the influence of these two effects needs to be separated in the experiment. The optical power of pulsed light is determined by two degrees of freedom: its pulse energy and its repetition rate. For repetition rates lower than the inverse dead time of the APDs no pulses are lost during the inactive time of the APDs. A repetition frequency of 1 MHz provides pulses which are further separated in time than the APD dead time. Thus we expect that the count rates reflect directly the quantum properties of (5) for variable attenuation.

Figure 3 shows the detected count rates against the optical transmission with detected values ranging from 124 kcnt s^{-1} up to 571 kcnt s^{-1}. For low transmission levels the linear

fit included in the figure indicates that a linear behaviour is again observable. For higher transmission the observed count rates are significantly lower than those predicted by the linear fit. Taking into account the repetition frequency $f_{rep} = 1$ MHz and the photon-number statistics of a coherent state we can estimate the mean photon-number according to (5). We find an effective mean photon-number of $|\eta_{det}\alpha|^2 = 0.836$, with a dark-count level of 9.9 kcnt s^{-1}. While the fitting accuracy of ± 0.002 is very good, the absolute precision of the $|\alpha|^2$ determination suffers again from the missing information of the absolute quantum efficiency of the APDs.

The fitted dark-count level of 9.9 kcnt s^{-1} is much higher than the absolute dark counts of the APDs; however, the fitted dark-count levels are strongly influenced by stray light. These should not be confused with the values obtained for a completely shielded APD during the characterization of the APDs. The measurement results along with the corresponding fitting curves are shown in figure 3. The graphs according to (5) provides excellent agreement with the measured data. The linear fitting demonstrates that for count rates up to ≈ 230 kcnt s^{-1} APDs can be linearly approximated. For higher mean photon-numbers the non-photon-number resolving nature of the detection process becomes eminent and the number of counts does not correspond directly to the number of photons any more. Nevertheless, the count rates confirm nicely the Poissonian photon-number distribution of coherent light and our modelling of the APD response such that an effective mean photon-number can be retrieved with high accuracy if Poissonian statistics are presumed.

4.3. Pulsed light at constant pulse energy

If the energy of a single pulse is kept constant, the mean optical power of a pulsed system can also be adjusted by varying the repetition frequency of the laser. Though, the number of photons per pulse is solely determined by the pulse energy. Hence increasing the mean optical power by going to higher repetition rates corresponds to preparing a larger sample of quantum states with equal properties. In this experimental configuration nonlinear changes in the count rates cannot are not related to different photon-number properties, but must be attributed to the limited speed of APD detection.

If the repetition time, which is the inverse repetition frequency, is greater than the dead time of the detector, no pulses are masked by a blocked detector. For low pulse energies we expect with (1) a linear dependency of the count rate on the repetition frequency. For higher repetition frequencies the detector might be in the recovery phase from a previous pulse when a new pulse arrives. This pulse is not counted; we need to introduce a correction for the count rate such that follows

$$R_{cnt} = f_{rep}\eta_{APD}(1 - P_0)C_{puls} + R_{dark}, \tag{7}$$

where the additional correction C_{puls} is now included. Note that C_{puls} is not a constant factor, but depends itself on the repetition rate and the photon statistics.

An event will not be registered if the APD is blocked by a previous detection event. The relevant time scale for the APDs being blocked is their dead time. In order to determine whether a pulse can be detected we need to calculate the probability that no APD counts occurred prior to a potential detection event during one dead-time interval. The repetition rate defines a time grid for possible detection events: for $\frac{T_{dead}}{n} \geqslant T_{rep} > \frac{T_{dead}}{n+1}$ we find n time slots, which fit into the detector dead time. These must be considered for calculating C_{puls}. We define p_γ as the probability of an APD CLICK for low repetition rates $p_\gamma = \eta_{APD}(1 - P_0)$, which also depends on the input photon-number statistics. The probability of n consecutive
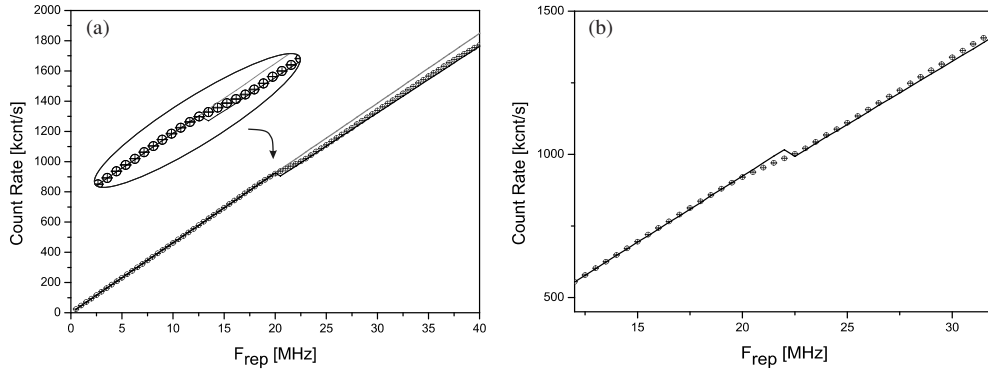
Figure 4. The measured count rates for pulsed light at constant pulse energy are plotted against the laser repetition frequency. (a) The linear fit (light grey) shows the linearity regime up to approximately 15 MHz, while for higher count rates the correction needs to be applied (black line) to explain the nonlinear count-rate response. (b) The simulated count-rate response (black line) reproduces the measured data, if dead-time effects are taken into account. For both graphs the errors in the measured count rates are too small to be visible.

time slots being empty—and thus the detector being ready to fire for a consecutive pulse—is then given by $(1 - p_\gamma)^n$. This defines the correction factor to first order as

$$
C_{\text{puls}} = \begin{cases} 1 & \text{if} \quad T_{\text{dead}} < \dfrac{1}{f_{\text{rep}}} = T_{\text{rep}}, \\[2ex] 1 - p_\gamma & \text{if} \quad T_{\text{dead}} \geqslant T_{\text{rep}} > \dfrac{T_{\text{dead}}}{2}, \\[1ex] \vdots \\[1ex] (1 - p_\gamma)^n & \text{if} \quad \dfrac{T_{\text{dead}}}{n} \geqslant T_{\text{rep}} > \dfrac{T_{\text{dead}}}{n+1}. \end{cases} \tag{8}
$$

We would like to point out that this analysis requires low p_γ. We neglect effects arising from the possibility that pulses can get registered if more than one potential detection event fall within twice the dead time before the considered APD count. For higher p_γ such higher order effects must be taken into account and (8) overestimates the actually necessary correction.

For intervals of the repetition frequency that are defined by multiples of the inverse dead time, the correction factor does not change. We expect linear dependencies within the defined segments. According to (8) the different intervals are interrupted by a transition region with a step function. While we were able to reproduce the predicted linearity regimes for repetition frequencies up to 80 MHz, we restrain our plots to the first two linearity regions in order to improve readability. In figure 4, we plot the measured count rates against the laser repetition frequency. To cope with power fluctuation we renormalized with respect to the pulse energy at a repetition frequency of 1 MHz. Two linearity regimes can be identified in the intervals (0.5 MHz; 15 MHz) and (23 MHz; 36 MHz).

The first linearity regime is valid to repetition rates up to nearly 20 MHz, showing count rates of more than 800 kcnt s^{-1}. If we apply the correction factor of the APD data sheet in a naive manner also for pulsed light, it would suggest that significant corrections of up to 10% are needed to correct for the real count rates. However, the observed linearity thus rules out the necessity and applicability of the standard APD correction to pulsed systems. In contrast, our results show that for pulsed light we can use APDs without any objections for repetition

rate up to their inverse dead times. In the transition region between the two linearity regimes a drop of count rates can be observed and the transition regime covers the inverse dead time of the detectors.

We use a binary model for the correction: it takes effect at a certain time and does not take into account dead-time jitter. Thus in the transition regime itself the measured data differs from the corrected plot. For the following linearity regime we find good agreement again with the measured data again. We apply our correction factor according to (8) to the linear fit, which is included in figure 4. The break-in of count rates is clearly accounted for, although the correction slightly underestimated the resulting count rate. After-pulsing and dark-count effects scale linearly with the repetition frequency and thus result in an overestimation of p_γ. Eventually, this leads to an overestimate of the necessary correction, which can be understood by recalling that our model is to first order and actually neglects more than two consecutive pulses. As already mentioned it is only valid for low probabilities and relies on the knowledge of the correct value of p_γ. Still, our results demonstrate clearly the linearity of APDs when operated at frequencies below their inverse dead time at constant pulse energy and the correction estimated from p_γ and (8) is actually in good agreement with the experimental data up to a small discrepancy.

4.4. Simulation

We designed a Monte Carlo simulation to validate the predicted influence of the APD dead time. We included cw-light sources by modelling the cw count rates as a pulsed system with infinite repetition frequency. A crucial point in this approach is to carefully calculate the pulse energy in order to keep the average optical power constant. For increasing repetition rates the pulse energy must be adjusted using the Poissonian photon-number distribution of coherent light. We simulated the pulsed case first, in order to verify our simulation with the measured data. The simulation reproduced the measured linearity regimes and transition regions. In figure 4, we compare the measured count rates for a simulation using similar parameters as given in the experiment. Since we used a binary model for the initiation of the correction, the transition region shows a small deviation from the simulation. The linearity regimes are reproduced well by the simulation, but the correction is also overestimated. Since the simulation was initialized with an initial p_γ taken from the measurement data, this indicates again that after-pulsing and dark-count contributions actually caused the overestimation of this crucial parameter. The significantly lower deviation between simulation and our analytical model arise from some higher order contributions. Next, we increased the repetition frequency and observed a convergence of the correction factors for high repetition frequencies. These reproduce the shape of the detected correction factor against counts curve in the cw-case. An offset is introduced due to insufficient measurement accuracy of the power meter, which is needed for absolute calibration.

The performed experiments in combination with the simulated results provide a complete understanding of the APDs and show the independence of the detection quantum efficiency from the count rate. Corrections only arise from the binary nature of the detector and detector dead time, which might be mistaken as a change in detection efficiency at first glance. Thus for quantum information applications data rates up to the inverse dead time are reasonable.

5. Application in time-multiplexed detection

TMD measurements rely on the fact that APDs can be driven at rates defined by the inverse of their dead times while showing no drop of their quantum efficiencies. We have experimentally

confirmed these assumptions with the results presented in the previous sections. The concept of TMDs offers the distinct advantage of low experimental complexity while the speed of operation is only limited by the minimum time APDs require to measure consecutive detection events.

In TMD detection, the photon-number resolution is achieved by using temporal modes for 'photon chopping': a pulse signal which is under investigation is split into several pulses, which get partially delayed in time and detected with individual binary detectors. For the practical realization of a TMD an important issue is the setting of the base delay between expected detection events. This must be at least the APD dead time in order to prevent the temporal modes from being masked by the APD dead time. To test the applicability of TMDs for higher bit rate applications we implemented a two-stage TMD with eight outgoing modes. We actually chose a delay around $\Delta T_{\text{base}} = 100$ ns to restrain also after-pulsing influences. Additionally to previous realizations, we implemented an electronic gating to inhibit noise contributions and a computer-controlled data acquisition system. The data acquisition speed above 2 MHz in our system is only bounded by physical constraints, i.e. four times the base delay.

For light with non-negligible higher multi-photon contributions multiple photons may still be transmitted into the same mode when leaving the TMD fibre network. They do not get discriminated by the subsequent detection with the binary APDs, resulting in a lower count rate than the actual photon-number of the input light. While this introduces an uncertainty for one single-shot measurements, for ensemble measurements this experimental imperfection can be included in the post-processing of the data analysis for studying photon-number statistics. As shown previously (Achilles *et al* 2004) a photon-number distribution $\vec{\rho}$ transforms to click statistics $\vec{p}$ according to

$$\vec{p} = \mathbf{C}\vec{\rho}, \tag{9}$$

where the convolution matrix $\mathbf{C}$ accounts for the probabilities of n incident photons resulting in $0, \ldots, n$ detectors firing.

Losses in the optical system and the non-unity detector efficiency also result in lower click rates than photons in the initial pulse. All losses in the system can be combined in an effective single-beam splitter in front of the fibre network (Silberhorn *et al* 2004, Achilles *et al* 2006) and represented by an additional matrix $\mathbf{L}$. The initial photon-number distribution is then retrieved from the detector click statistics using an ordinary matrix inversion:

$$\vec{\rho} = \mathbf{L}^{-1}\mathbf{C}^{-1}\vec{p}. \tag{10}$$

While the effects of losses and the usage of the TMD detection for the characterization of arbitrary photon statistics are thoroughly investigated in previous work (Achilles *et al* 2006, 2004), we concentrate on the influence arising due to the convolution. We utilized an optical setup similar to the experiments with APDs shown in figure 1 to feed coherent light of different power levels into the TMD. We would like to point out that that the usage of coherent light in these studies is crucial in order to be able to distinguish effects arising from attenuating the input-state statistics from distinct characteristics, which are intrinsic to the TMD detector response. As stated earlier, attenuation only changes the mean photon-number of the Poissonian statistics while effects on the shape of the photon-number distribution caused by introducing losses are eliminated. The mean number of photons depends linearly on the attenuation. Though in analogy to a single APD being illuminated with more than a single photon per pulse, masking of higher photon-numbers due to photons, which stay together in one outgoing mode, is expected.

In figure 5, we plot the mean number of clicks before and photons after deconvolution against the applied attenuation. Similar to the result of figure 3 a linear dependency is visible
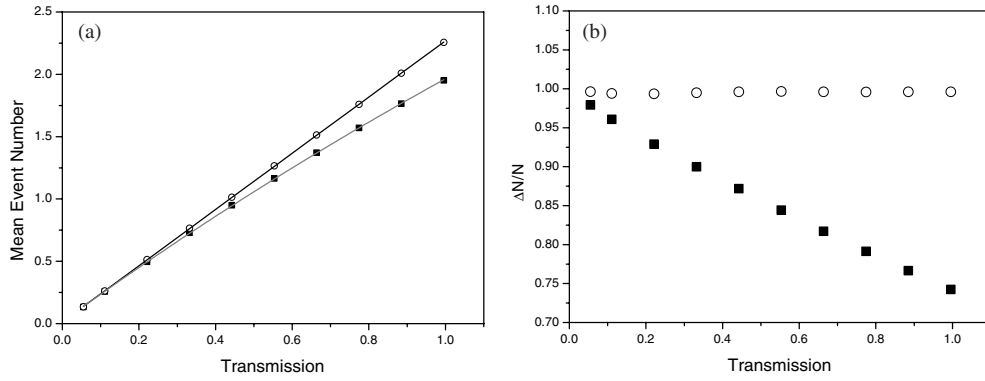
Figure 5. (a) The mean number of clicks (■) and the mean number of photons after deconvolution (○) are plotted against the transmission. For the deconvoluted data the expected linear fit holds over the full range of transmission, while for the click data nonlinear behaviour is visible for higher transmission. The clicks follow (12), which can be verified looking at the light grey fitting line. (b) For the deconvoluted data (○) the Mandel Q-parameter against the transmission shows the expected value of 1 for all transmission levels. For the click data Mandel Q-parameters less than 1 falsely indicate non-Poissonian nature.

for low transmissions, corresponding to a low mean number of clicks or photons, respectively. For higher click rates a significant deviation from the linear fit develops, while the deconvoluted data increases linearly with increasing transmission. More photons are distributed into the same time slot, triggering less clicks than photons in the pulse. Thus the raw data will give an underestimate of the mean photon-number, which can be modelled by assuming k perfect beam splitters in the fibre network. The coherent input state with the mean photon-number $|\alpha|^2$ is split into 2^k modes with corresponding mean photon-numbers $|\alpha|^2/2^k$. For each mode the detection rate is given by (5) and summing these rates yields the effective count rate after the fibre network as

$$\tilde{R}_{cnt} = \sum_{i=1}^{2^k} f_{rep} \left(1 - \exp\left(-|\eta|^2 \frac{|\alpha|^2}{2^k}\right)\right) + \tilde{R}_{dark}. \tag{11}$$

The expected mean number of clicks is obtained by dividing by the repetition frequency and for a TMD with eight time bins we expect a mean number of clicks

$$\bar{c} = 8 \left(1 - \exp\left(-|\eta|^2 \frac{|\alpha|^2}{8}\right)\right) + \frac{\tilde{R}_{dark}}{f_{rep}}. \tag{12}$$

In figure 5(a), we also display a fit of this expected click rate to the data, which shows perfect correspondence for values of $\tilde{R}_{dark} = 16 \pm 3$ kcnt s^{-1} and an effective $|\alpha|^2 = 2.232 \pm 0.006$. The graphs indicate that we are able to demonstrate experimentally convolution utilizing well-known quantum states. Moreover, the use of the deconvolution method to retrieve the original statistics is experimentally verified by retrieving the linear dependence.

The value of the Mandel Q-parameter $\sigma^2/\bar{n}$ is often used to characterize the non-classicality of a photon-number distribution(Mandel and Wolf 1995). In figure 5, we plot the Q-parameter against the variable transmission and compare the results for the raw click statistics with the deconvoluted data. A Poissonian distribution of a coherent state always results in a Q-factor of 1. Our experimental data confirm this expected Q-factor for the deconvoluted data at all transmission levels. For low photon-numbers, i.e. transmission,

the raw data still show values near 1. This value, however, drops significantly below 1 for higher transmission rates, indicating falsely a non-Poissonian nature of the assumed photon-number statistics. Higher photon-numbers are more strongly affected by the decrease in clicks than lower photon-numbers. Thus the raw click statistics show non-Poissonian features indeed, which must not be mistaken for non-Poissonian photon-number statistics. From our measurements—depicted in figure 5(b)—we ascertain that the deconvolution of the measured click statistics is essential to obtain correct photon-number statistics when utilizing TMD detection for quantum state characterization. Contrariwise, we demonstrated experimentally that using the deconvolution matrix approach the correct statistics can be deduced.

Since the Q-parameter is regarded as an indicator for the non-classicality of light, it is crucial to consider the impact of detectors on measured outcomes. At first glance—without taking detector saturation into account—a source might appear to exhibit non-classical Q-parameters which might then be falsely interpreted as photon-number squeezing. In our parameter regime, we demonstrated that the TMD detector saturation can be perfectly compensated by applying the deconvolution in the data post-processing. This is verified by the constant Q-factor of 1 after the application of the deconvolution. The computation power for calculating the convolution matrix numerically rises exponentially with the number of photons resolved by the detector. For more than eight TMD bins only the idealized case of perfect splitting ratios can be easily calculated analytically (Fitch *et al* 2003). Thus we investigated the effects of using symmetric splitting ratios for deconvoluting simulated data with unbalanced splitting ratios. We found that the convolution matrices are surprisingly independent of the splitting ratios of the beam splitters used in the TMD fibre network—which, in turn, enables the extension of the TMD to higher numbers of bins without any major problems in the mathematical treatment. In practice, the deviations due to convolution effects will be much less than errors caused by imperfections in the optical loss calibration.

6. Conclusion and discussion

In summary, we characterized APDs in the context of testing the limits of their application in quantum information processing. A major challenge is the extremely precise calibration of the used attenuation, which contributes most to the errors of the experiment. In particular, the cw-light measurements require optical power spanning several orders of magnitude in order to start measuring in the linear regime, while getting significant nonlinearities at higher power levels. With the simulation being extremely sensitive to errors in the calibration, better methods for even more precise calibration are needed and should close the gap between simulation and measured correction factors.

By using pulsed light we could differentiate two sources of nonlinear APD response: intensity and pulse repetition frequency. For quantum communication at high data rates an essential characteristic of an APD is its dead time where we verified for repetition frequencies up to its inverse dead time a linear APD behaviour. With dead times of 50 ns for commercially available APD modules this allows for data rates up to 20 MHz.

An important application of APDs is the TMD, where we complemented the detector description by verifying experimentally that saturation effects can be compensated in the post-processing data analysis. We can now operate the TMD at the data acquisition speed limit given by the APDs dead time. This is a powerful tool to quickly characterize quantum states in the photon-number bases allowing the collection of large number of statistical data in short measurement time. We expect that this provides the basis for photon-number-based characterization of highly non-classical quantum states where the number of recorded data points during the stability of an optical setup becomes crucial.

Acknowledgment

References

Achilles D, Silberhorn C, Sliwa C, Banaszek K and Walmsley I A 2003 *Opt. Lett.* **28** 2387–9
Achilles D, Silberhorn C, Sliwa C, Banaszek K, Walmsley I A, Fitch M J, Jacobs B C, Pittman T B and Franson J D 2004 *J. Mod. Opt.* **51** 1499–515
Achilles D, Silberhorn C and Walmsley I A 2006 *Phys. Rev. Lett.* **97** 043602
Bienfang J *et al* 2004 *Opt. Exp.* **12** 2011
Banaszek K and Walmsley I A 2003 *Opt. Lett.* **28** 52–4
Cabrera B, Clarke R, Colling P, Miller A, Nam S and Romani R 1998 *Appl. Phys. Lett.* **73** 735
Castelletto S, Degiovanni I P and Schettini V 2006 *Preprint* quant-ph/0601102
Fitch M J, Jacobs B C, Pittman T B and Franson J D 2003 *Phys. Rev.* A **68** 043814
Fujiwara M and Sasaki M 2006 *Opt. Lett.* **31** 691–3
Gordon K, Fernandez V, Buller G, Rech I, Cova S and Townsend P 2005 *Opt. Exp.* **13** 3015
Grosshans F, van Assche G, Wenger J, Brouri R, Cerf N J and Grangier P 2002 *Nature* **421** 238–41
Hadfield R H, Stevens M J, Gruber S S, Miller A J, Schwall R E, Mirin R P and Nam S W 2005 *Opt. Exp.* **13** 10846–53
Hansen H, Aichele T, Hettich C, Lodahl P, Lvovsky A I, Mlynek J and Schiller S 2001 *Opt. Lett.* **26** 1714
Hirano T, Yamanaka H, Ashikaga M, Konishi T and Namaki R 2003 *Phys. Rev.* A **68** 042331
Kim J S, Takeuchi S, Yamamoto Y and Hogue H H 1999 *Appl. Phys. Lett.* **74** 902–4
Klyshko D N 1977a *Sov. J. Quantum Electron.* **10**
Klyshko D N 1977b *Kvantovaya Elektron.* **4** 1056–62
Kok P and Braunstein S L 2001 *Phys. Rev.* A **63** 033812
Lance A M, Smyl T, Sharma V, Weedbrook C, Ralph T C and Lam P K 2005 *Phys. Rev. Lett.* **95** 180503
Lorenz S, Rigas J, Heid M, Andersen U L, Lütkenhaus N and Leuchs G 2006 pp 1–12 *Preprint* quant-ph/0603271v1
Mandel L and Wolf E 1995 *Optical Coherence and Quantum Optics* (Berlin: Springer)
Paul H, Torma P, Kiss T and Jex I 1996 *Phys. Rev. Lett.* **76** 2464–7
Penin A N and Sergienko A V 1991 *Appl. Opt.* **30** 3582–8
Rarity J G, Ridley K D and Tapster P R 1987 *Appl. Opt.* **26** 4616–9
Raymer M G, Cooper J, Carmichael H J, Beck M and Smithey D T 1995 *J. Opt. Soc. Am.* B **12** 1801–12
Rosenberg D, Lita A E, Miller A J and Nam S W 2005 *Phys. Rev.* A **72** 019901
Silberhorn C, Achilles D, U'Ren A B, Banaszek K and Walmsley I A 2004 *Proc. 7th Int. Conf. on Quantum Communication, Measurement and Computing QCMC 2004 (Glasgow, 25–29 July 2004)*
Smithey D T, Beck M, Raymer M G and Faridani A 1993 *Phys. Rev. Lett.* **70** 1244
Somani S, Kasapi S, Wilsher K, Lo W, Sobolewski R and Gol'tsman G 2001 *J. Vacuum Sci. Technol.* B **19** 2766–9
SPCM-AQR Single Photon Counting Module Datasheet 2005 PerkinElmer Inc. Vaudreuil, QC, Canada
Takesue H, Diamanti E, Langrock C, Fejer M M and Yamamoto Y 2006 *Opt. Exp.* **14** 9522–30
Thew R T, Tanzilli S, Krainer L, Zeller S, Rochas A, Rech I, Cova S, Zbinden H and Gisin N 2006 *New J. Phys.* **8** 32
Ware M and Migdall A 2004 *J. Mod. Opt.* **51** 1549–57
Wenger J, Fiurasek J, Tualle-Brouri R, Cerf N J and Grangier P 2004 *Phys. Rev.* A **70** 053812
Wenger J, Tualle-Brouri R and Grangier P 2004 *Opt. Lett.* **29** 1267–9
Zambra G, Andreoni A, Bondani M, Gramgna M, Genovese M, Brida G and Paris M G A 2005 *Phys. Rev. Lett.* **95** 063602
Zavatta A, Bellini M, Ramazza P L, Marin F and Arecchi F T 2002 *J. Opt. Soc. Am.* B **19** 1189–94